Transient Loading Effects on Pore Pressure Generation and the Response of Liquefiable Soils

Steven L. Kramer[1] and Samuel S. Sideras[2]

[1] 132E More Hall, University of Washington, Seattle, WA 98195-2700, USA
kramer@uw.edu
[2] Shannon & Wilson, 3990 Collins Way, Suite 100, Lake Oswego, OR 97035, USA
sam.sideras@shanwil.com

Abstract. Like ground motions, the loading applied to potentially liquefiable soils in earthquakes is complex and unique. Conventional procedures for characterizing liquefaction hazards represent seismic loading in simplified manners that do not account for characteristics that can influence pore pressure generation and potential ground deformation. This paper presents the results of cyclic direct simple shear tests performed with transient, irregular loading derived from recorded earthquake ground motions. Data from these tests show the influence of the order in which individual pulses of shear stress occur on generated pore pressure and provide insight into limitations of evolutionary intensity measures based on time integration to provide efficient predictions of liquefaction. The form of a new intensity measure for triggering of liquefaction is proposed and calibrated on the basis of available data. The response of cyclic simple shear specimens subjected to transient loading superimposed upon static shear stresses is also illustrated and comments on existing procedures for estimation of the adjustment factor, K_α, are provided.

Keywords: Liquefaction, pore pressure, loading, relative density

1 Introduction

Soil liquefaction has caused significant damage to the natural and built environment in many historical earthquakes and has been a topic of intense geotechnical engineering research for nearly 60 years. Over that period of time, many studies have taken place to understand the mechanical behavior of liquefiable soils and to develop useful and practical procedures to assess liquefaction hazards. Most of the research on soil liquefaction has been oriented toward evaluation of soil resistance to the triggering of liquefaction and, more recently, to prediction of its consequences. Both triggering and consequences, however, are strongly influenced by the loading imposed on liquefiable soils and less attention has

historically been paid to this aspect of the problem. This paper focuses on characterization of loading and its effects on liquefiable soils.

2 Ground Motions and Liquefaction Loading

The seismic loading imposed on a liquefiable soil deposit is related to the characteristics of the ground motions that propagate through that deposit. Ground motions are unique and the response of a liquefiable soil deposit can be sensitive to many details of their specific characteristics. A 60-second ground motion recorded at 200 Hz will have 12,000 acceleration values each of which provides potentially important information about the motion's ability to generate pore pressure and produce permanent strain in an element of a liquefiable soil deposit. Ground motions are typically characterized by a relatively small number of intensity measures (*IM*s) that are intended to reflect their amplitudes, frequency contents, and durations since each of those factors can influence the seismic response of physical systems (structures and soil deposits) of interest. The degree to which these characteristics influence response, damage, and loss, however, is problem-specific. Thus, characterization of ground motions for the purpose of estimating liquefaction potential and the consequences of its triggering becomes important. The *IM* historically used for characterizing earthquake loading imposed on liquefaction-susceptible soils is peak ground acceleration, due largely to its close relationship to peak shear stress at the relatively shallow depths at which liquefaction has most commonly been observed in the field. Early experimental research showed, however, that pore pressure generation also depends on the number of cycles of loading applied to the soil in laboratory tests. To eliminate the need for a parameter related to number of loading cycles in addition to peak ground acceleration in the characterization of loading, other intensity measures have been proposed for use in liquefaction triggering relationships. Most of these alternative *IM*s have been evolutionary in nature, i.e., they have consisted of measures that are integrated with time over the duration of a ground motion. Such intensity measures, such as Arias intensity [16], cumulative absolute velocity and variations thereof [19], and dissipated energy [10, 18, 27], increase with time and reflect the amplitude, frequency content, and duration of a ground motion.

Early research on liquefaction made use of laboratory testing for evaluation of liquefaction resistance, which was interpreted in terms of cyclic shear stresses. Cyclic triaxial tests were commonly used, although cyclic direct simple shear testing is becoming more common now due to its closer correlation to the type of deformation usually experienced by liquefiable soils subjected to vertically propagating shear waves. Cyclic testing has nearly always subjected soil specimens to uniform harmonic loading – a series of harmonic loading cycles of constant shear stress amplitude applied at constant frequency. These tests have provided great insight into the effects of factors such as soil density, initial effective stress, shear stress amplitude, number of loading cycles, etc. that strongly affect the resistance of a soil to triggering of liquefaction.

The type of transient loading produced by actual earthquake shaking, however, is very different than that used in typical laboratory testing programs. The shear stress histories

imposed on soils by earthquakes are highly non-stationary, meaning that their amplitudes and frequency contents change over the duration of shaking. The number of loading cycles is difficult to predict for a given earthquake but is expected to increase with increasing ground motion duration. Since ground motion duration is known to increase with increasing earthquake magnitude, the concept of "equivalent" loading cycles was developed [29]. This concept held that the pore pressure generated by a transient loading history would be equivalent to that generated by a certain number of uniform harmonic loading cycles at a reference amplitude and required definition of both the reference loading amplitude and the corresponding number of loading cycles.

Characterization of ground motions for liquefaction becomes even more complex when the effects of sloping ground are considered. In such cases, the cyclic shear stress imposed by earthquake shaking is superimposed on constant static shear stresses with the result that the soil is subjected to asymmetric loading that influences pore pressure generation and causes permanent strain to develop in a preferential direction.

3 Pore Pressure Response to Cyclic Loading

The contractive tendency of soils at relatively low shear strain levels cause pore pressures to increase in saturated soils subjected to cyclic loading. This tendency is at the heart of the soil liquefaction problem and establishing the rate at which pore pressures are generated is key to the prediction of liquefaction potential. The level of contraction that occurs in liquefiable soils is related to the shear strain experienced by the soil, and undrained cyclic testing of soils has established the close relationship between pore pressure and cyclic strain amplitude [8]. Pore pressure generation can then be viewed as a largely kinematic process, i.e., one that depends on the relative movement of soil grains with respect to each other. Prediction of that relative movement, i.e., of shear strain levels, is very difficult. As a result, pore pressure generation, and the liquefaction it can produce, are generally related to the cyclic stresses induced in the soil by earthquake shaking. Laboratory tests are usually performed under stress-controlled conditions.

3.1 Uniform Harmonic Loading

Laboratory tests on liquefiable soils have historically been performed using uniform (constant-amplitude) harmonic loading, typically at a constant frequency of 1 Hz. Plots of cyclic shear stress, usually normalized by initial effective stress, σ'_{v0}, in the form of a cyclic stress ratio, *CSR*, versus the number of loading cycles required to trigger liquefaction are often referred to as cyclic strength curves. Figure 1 shows cyclic strength curves for reconstituted samples of a clean sand at three relative densities. The curves show that the cyclic stress ratio required to trigger liquefaction decreases with increasing number of loading cycles and increases with increasing relative density, behaviors that are intuitive, well demonstrated, and widely accepted. The relationship between the cyclic resistance and the number of loading cycles is particularly important as it indicates that liquefaction resistance, for a given soil of a given density, is influenced by both amplitude and number

of loading cycles. The rate of pore pressure generation in constant-amplitude tests has been shown to follow a repeatable pattern (Figure 2) of starting rapidly, slowing down, and then speeding up as initial liquefaction (pore pressure ratio, r_u = 100%) is approached. The first phase likely involves some degree of particle reorientation as tenuous contacts are broken, the second involves incremental generation of pore pressure with a more stable particle structure, and the third involves particle reorientation during dilation as the effective stress path approaches and crosses the phase transformation line. As the soil dilates, the particles reorient themselves into a structure that efficiently resists shear stress in the applied direction; upon stress reversal, however, that structure is inefficient for resisting shear in the new direction, which increases its tendency to contract and generate pore pressure until it begins to dilate in the new direction.

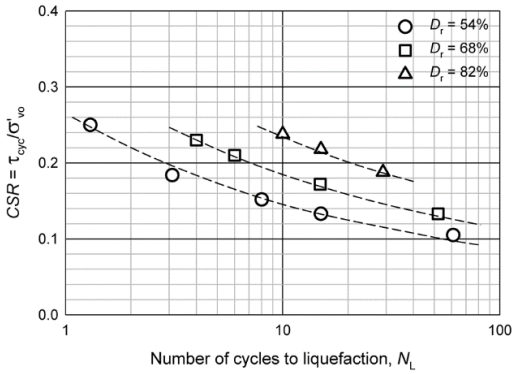

Fig. 1. Variation of number of cycles required to trigger liquefaction of Monterey No. 0 sand with amplitude of applied loading for soils of different relative density (after [8]).

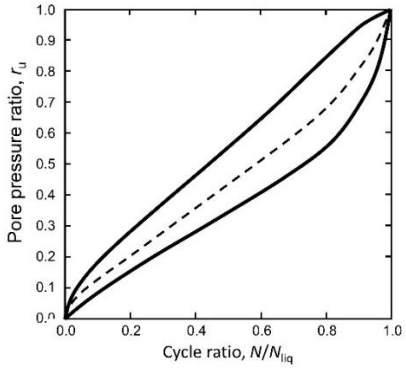

Fig. 2. Variation of pore pressure ratio with cycle ratio for constant-amplitude harmonic loading (after [8]).

In the presence of a static shear stress, τ_{static}, as would exist in the field under sloping ground or in the vicinity of structures, the loading that drives pore pressure generation has both static and cyclic components. This situation is relatively easily modeled in laboratory tests by applying uniform harmonic loading to a specimen to which a static shear stress has been applied; the result is a harmonic loading history in which the same number of loading cycles is applied but of shear stress amplitudes that are larger in one direction than the other. Such tests have shown that the interaction of static and cyclic stresses is complex and that the presence of static shear stresses can increase or decrease triggering resistance depending on soil density. This behavior is accounted for in triggering analyses by a static shear stress adjustment factor,

$$K_\alpha = \frac{CRR_\alpha}{CRR_{\alpha=0}} \tag{1}$$

where $\alpha = \tau_{static} / \sigma'_{vo}$, which the cyclic resistance for level ground conditions ($\alpha = 0$) is multiplied by to account for the effect of the static shear stress. Values of $K_\alpha > 1.0$ increase liquefaction resistance and values less than 1.0 decrease it. Figure 3 shows four proposed K_α relationships, each of which indicate that static shear stresses decrease the liquefaction resistance of loose sands and increase it in dense sands. With the transient loading applied by actual earthquakes, however, the existence of a static shear stress causes a reduction in the number of loading cycles that result in reversals of shear stress in addition to a reduction in the amplitudes of the reversed cycles.

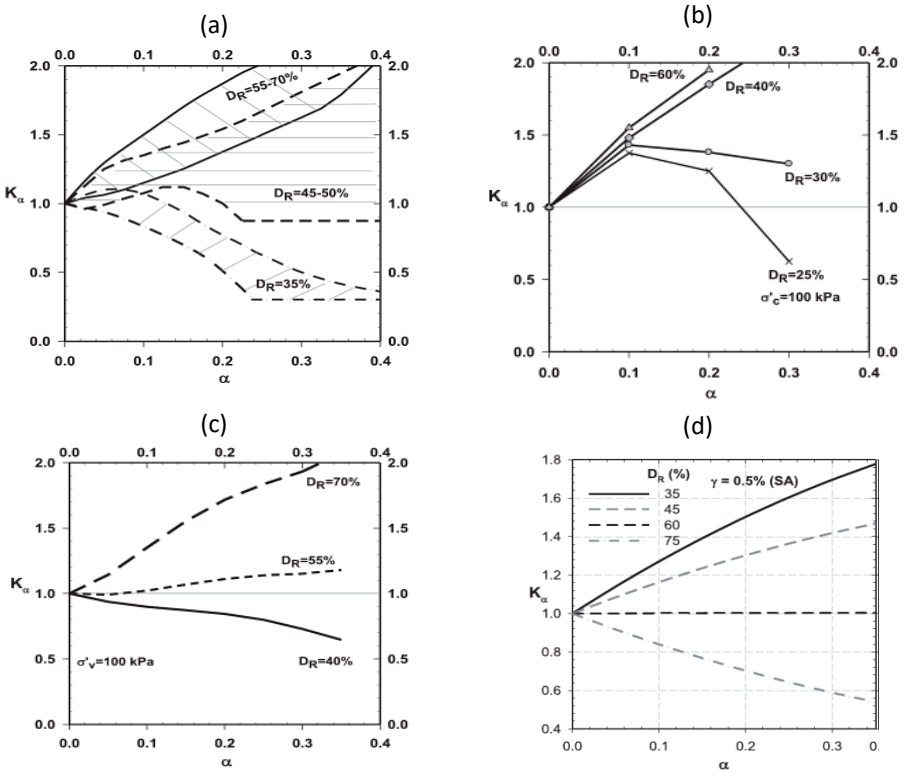

Fig. 3. Existing models for initial shear stress adjustment factor, Ka: (a) Seed and Harder [30]; (b) Vaid et al., [35]; (c) Boulanger [4]; and (d) Cetin and Bilge [6].

3.2 Transient Loading

Several investigators have performed cyclic loading tests with irregular (variable amplitude) loading. Ishihara and Yasuda [14, 15] performed cyclic triaxial tests using

loading histories scaled in proportion to accelerograms measured in the basement of the Kawagishi-cho apartment building in the 1964 Niigata earthquake. The tests showed irregular generation of pore pressure with the largest increases being associated with the highest axial stress pulses, and tests performed with reversed polarity showed significant differences in pore pressure development, presumably due to differences in the loading histories relative to the compression/extension stress states inherent in cyclic triaxial testing. Tatsuoka and Silver [33] performed cyclic simple shear tests with uniform and irregular loading and focused on the development of strain following initial liquefaction. Wang and Kavazanjian [36] performed cyclic triaxial tests with the same numbers of smaller and larger amplitude cycles but reversed in order and found that the order of loading influenced the rate and magnitude of generated pore pressures. More recent investigations [2, 3, 22, 26] have largely focused on the potential of energy-based intensity measures for prediction of liquefaction potential. Transient loading tests with static shear stresses are not available in the literature.

4 Intensity Measures for Liquefaction

The triggering of liquefaction is influenced by ground motion characteristics and hence by the ability of ground motion intensity measures to represent the characteristics that are most strongly influence pore pressure generation. Ideally, a ground motion intensity measure would have a unique relationship to pore pressure generation. Because such an intensity measure does not exist, an intensity measure that best predicts pore pressure is sought. The notion of what constitutes "best" is usually expressed in terms of the "efficiency" [31], "sufficiency," and "predictability" of the intensity measure. Efficiency is a measure of the uncertainty with which a measure of response can be estimated for a given value of the intensity measure; an efficient *IM* for liquefaction would be one that the generation of pore pressure is closely related to, i.e., one for which the uncertainty in pore pressure given *IM* ($\sigma_{r_u|IM}$) would be low. Sufficiency is a measure of the completeness with which an *IM* characterizes the ground motion; a sufficient *IM* for liquefaction would be one for which no additional information about the motion would improve its correlation to pore pressure generation. Finally, predictability is a measure of how precisely the value of an *IM* can be predicted for a particular earthquake rupture scenario; a predictable *IM* would have a low standard error, i.e., $\sigma_{\ln IM}$, in a predictive ground motion model.

The laboratory data described in the preceding section clearly shows that an *IM* based solely on the peak amplitude is not sufficient to characterize loading on a liquefiable soil. Since pore pressure builds up incrementally from cycle to cycle, the potential for triggering of liquefaction depends on both the amplitude and number of cycles of loading. Under the transient loading of an actual earthquake, the relationship between number of cycles and ground motion amplitude is complicated. The approach that underlies most current liquefaction triggering procedures is based, explicitly or implicitly, on representation of a transient loading history by a number of equivalent uniform loading cycles. This approach

is usually implemented in the form of a magnitude scaling factor that can be used to adjust the loading to account for duration effects.

4.1 Number of Loading Cycles

Various cycle-counting procedures have been proposed to identify the amplitude and number of cycles of uniform harmonic loading that are equivalent, in terms of pore pressure generation potential, to a given non-stationary shear stress history. Hancock and Bommer [12] provide an extensive review of procedures for computing numbers of equivalent loading cycles for structural and geotechnical purposes.

The number of loading cycles is important for problems, such as metal fatigue, where damage accumulates with each cycle of loading. In such problems, a given level of damage can be caused by a small number of large loading cycles or by a larger number of smaller loading cycles. Liquefiable soils, in which excess pore pressure builds incrementally in response to successive cycles of loading, are an example of materials in which "damage," in this case pore pressure generation, evolves over time. Seismic loading of liquefiable soils in actual earthquakes involves highly non-stationary loading cycles with a small number of high-amplitude cycles preceded and followed by many more cycles of lower amplitude; each of these cycles can potentially contribute to pore pressure generation but do so in a complex manner. As such, a defined number of loading cycles at an effective peak amplitude that considers the relative contributions of the various cycles is needed to properly characterize the pore pressure generation potential of the loading history.

The most basic procedures for characterizing numbers of equivalent cycles [24, 25] are based on the assumption that damage accumulates linearly, i.e., that the damage produced by each of a series of uniform amplitude loading cycles produces the same increment of damage. Miner's derivation was focused on high-cycle fatigue of aluminum alloys used in the aircraft industry and inherently assumed material linearity in which cumulative absorbed work, i.e., dissipated energy, is proportional to number of loading cycles. Under this assumption, the damage, D, done by n_i cycles of loading of amplitude S_i can then be expressed as

$$D = \sum \frac{n_i(S_i)}{N_i(S_i)} \tag{2}$$

where N_i is the number of uniform loading cycles at amplitude S_i required to cause failure. With this criterion, failure occurs when $D = 1.0$. The assumption of strict linearity can be relaxed, however, by assuming that the damage produced by each cycle is a power law function of its amplitude, i.e.

$$N(S) = aS^b \tag{3}$$

where a and and b are constants that reflect the intercept and slope of a log-log plot of S vs. N. Then, substituting Equation (2) into Equation (1), the damage caused by a number of uniform equivalent cycles, N_{eq}, of amplitude S_{ref} can be set equal to the damage produced by the set of variable amplitude cycles

$$\frac{N_{eq}(S_{ref})}{aS_{ref}^{b}} = \sum \frac{n_i(S_i)}{aS_i^{b}} \tag{4}$$

from which the equivalent number of cycles at the reference stress can be expressed as

$$N_{eq}(S_{ref}) = S_{ref}^{b} \sum \frac{n_i(S_i)}{S_i^{b}} \tag{5}$$

Since the intercept constant, *a*, cancels out in Equation (3), the slope constant, *b*, which describes the rate at which the amplitude required to cause failure decreases with increasing number of loading cycles, can be seen to strongly influence the number of equivalent cycles.

The concept of a number of equivalent cycles was originally applied to liquefaction problems by Seed et al. [29] using a modified version of the Palmgren-Miner cumulative damage hypothesis. The reference stress was generally taken as a fraction of the peak stress; for liquefaction purposes, this fraction has historically been taken to be 0.65. This approach allows the number of equivalent cycles to be obtained from experimental data that use uniform harmonic loading to establish the relationship between load amplitude and number of cycles to failure. Cycle counting schemes based on Palmgren-Miner damage theory treat all loading cycles equally regardless of the order in which they occur. In addition, Seed et al. [29] considered only loading cycles of amplitude greater than 30% of the peak amplitude to be capable of generating significant pore pressure.

Liu et al. [23] used the vector sum of two orthogonal horizontal acceleration histories and individual peak amplitude weighting factors based on both laboratory and field data to define numbers of equivalent cycles. Using a large database of recorded ground motions along with consideration of source, path, and site effects, predictive models for numbers of equivalent cycles based on laboratory, field, and lab/field data were developed. The models predict number of equivalent cycles as functions of magnitude, distance, and site condition (soil or rock) while accounting for near-fault effects and show that N_{eq} increases with both magnitude and distance.

Recognizing that softening due to pore pressure generation prior to the triggering of liquefaction produces significantly nonlinear behavior, Green and Terri [11] proposed a cycle-counting scheme based on dissipated energy. In this approach, the dissipated energy of the transient and uniform motions are equated. The number of equivalent cycles was taken as the ratio of the cumulative dissipated energy to the energy dissipated in one cycle of loading at the reference stress, i.e., as

$$N_{eq}(S_{ref}) = \frac{\sum \omega_i}{\left[\omega(S_{ref})\right]_{1\ \text{cycle}}} \tag{6}$$

where ω_i is the energy dissipated in the i^{th} cycle of loading and $\left[\omega(S_{ref})\right]_{1\ \text{cycle}}$ is the energy dissipated in one cycle of loading at $S = S_{ref}$. The energy-based N_{eq} increases with distance

in a manner similar to that of the Liu et al. [23] model at distances less than about 75 km beyond which it remains nearly constant as the diminishing ground motion amplitude balances the effect of increasing duration with distance. Notably, N_{eq} also decreases with depth for typical soil profiles.

Each of these cycle counting procedures accounts for the relative sizes of the individual pulses that comprise a transient loading history and each assigns a weight to each pulse's expected contribution to pore pressure generation. The weighting functions are nonlinear and some include a threshold, generally relative to the peak amplitude of the entire history, below which no contribution to pore pressure is assumed. In all cases, the order or sequence in which the pulses arrive at a given element of soil is not considered – each pulse is considered to contribute according to its amplitude independent of the preceding loading history.

4.2 Magnitude Scaling Factor

The concept of equivalent cycles was implemented into liquefaction potential evaluations by means of a magnitude scaling factor, *MSF*. Recognizing that numbers of equivalent cycles increased with increasing ground motion duration, and that ground motion duration was most strongly influenced by earthquake magnitude, Seed et al. [29] related N_{eq} to magnitude with a magnitude of 7.5 being assumed to produce 15 equivalent cycles of loading. In the simplified procedure for evaluation of liquefaction potential, the magnitude scaling factor is applied to the peak acceleration for the entire ground motion; as a result, the effective *IM* is *PGA*/*MSF*. The magnitude scaling factor can be defined as

$$MSF = \frac{CRR_M}{CRR_{M=7.5}} = \left(\frac{N_{M=7.5}}{N_M} \right)^b \tag{7}$$

Using a value of $b = 0.34$ as being representative of clean sands from laboratory tests and a relationship between magnitude and number of equivalent cycles (Figure 4), Idriss [13] proposed the relationship

$$MSF = 6.9 \exp(-M / 4) - 0.058 \leq 1.8 \tag{8}$$

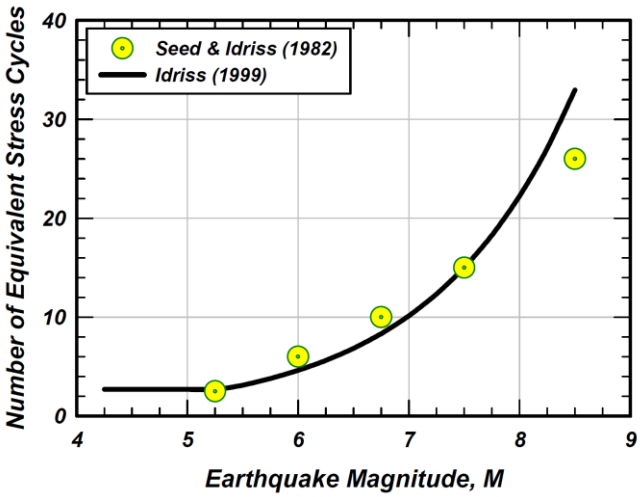

Fig. 4. Relationship between number of equivalent cycles and earthquake magnitude [5].

Boulanger and Idriss [5], noted that the slopes of laboratory cyclic resistance curves, represented by the *b*-parameter in Equations 2, 4, and 6, increased with increasing soil density [17] and proposed that

$$MSF = 1 + \left(MSF_{\max} - 1 \right)\left[8.64 \exp(-M / 4) - 1.325 \right] \tag{9}$$

where $MSF_{\max}$ is limited to being less than or equal to 1.8 for sand and 1.09 for clay and plastic silt and $MSF_{\max} = 1.09 + (q_{c1Ncs} / 180)^3 \le 2.2$ for CPT-based and $MSF_{\max} = 1.09 + (N_{1,60cs} / 31.5)^2 \le 2.2$ for SPT-based evaluations. Finding that the number of equivalent cycles for a given event depended on factors in addition to magnitude, Liu et al. [23] related a *CRR* scaling factor to number of equivalent cycles as

$$\ln CRR_{SF} = 1.3 - 0.41 \ln N_{eq} \tag{10}$$

The CRR_{SF} term can be used in a manner equivalent to *MSF* in the simplified method for evaluation of liquefaction potential. The variation of *MSF* and CRR_{SF} with magnitude from several triggering models is illustrated in Figure 5.

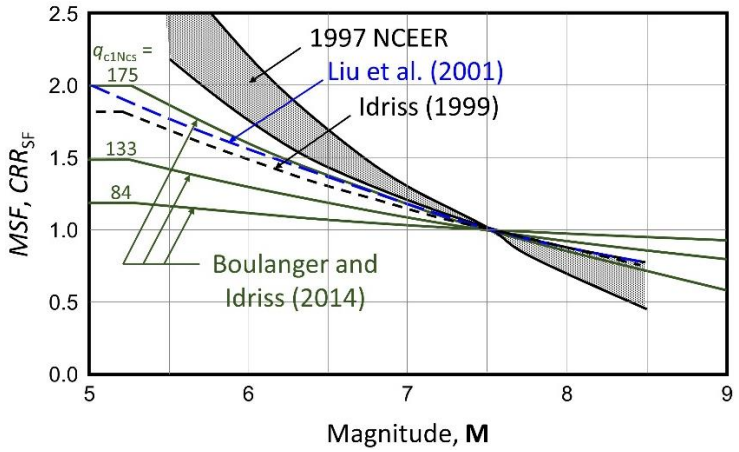

Fig. 5. Comparison of magnitude scaling factors.

5 Transient Loading Laboratory Testing Program

In order to explore alternative, and more efficient, intensity measures for evaluation of liquefaction potential under loading conditions more representative of actual earthquakes, a series of cyclic direct simple shear tests was performed on wet-pluviated samples of Nevada sand [20, 21, 32]. Two types of tests were performed: (a) tests with harmonic, constant-frequency loading of variable amplitude, and (b) transient loading derived from recorded earthquake motions.

5.1 Variable Amplitude Harmonic Loading

Figure 6 shows the results of a series of cyclic simple shear tests on specimens loaded with nine cycles of constant amplitude (*CSR* = 0.075) and one (either the 2nd, 4th, 6th, 8th, or 10th loading cycles) with twice that amplitude (*CSR* = 0.15). The applied loading produced relatively low pore pressure ratios so that phase transformation behavior was not exhibited. The pore pressure ratios after the first cycle of loading, which was identical in all tests, decreased exponentially with increasing specimen relative density. To reduce the effect of these differences, Figure 6(c) shows the pore pressure ratios normalized by their values after the first cycle of loading (which was identical in all tests). The results show that (a) the increment of pore pressure response prior to the large cycle was generally consistent for all specimens (and consistent with the behavior shown in Figure 2), (b) the large cycle produced a significantly larger pore pressure increment than the smaller cycles that preceded it, (c) very little additional pore pressure was generated by the lower-amplitude cycles that followed the large cycle even though cycles of the same amplitude had produced significant pore pressures before the large cycle, and (d) the final pore pressures were

influenced by the order of the loading cycles. These results suggest that the generation of pore pressure is influenced by both the order of the loading cycles and the maximum level of loading that a specimen has been subjected to.

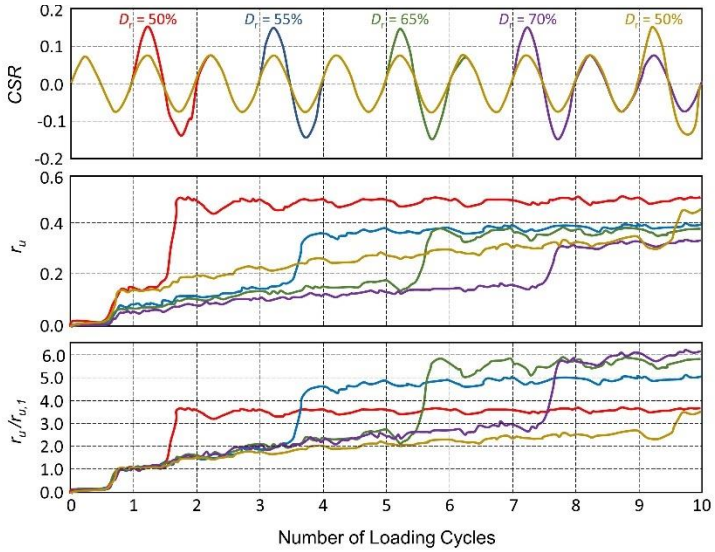

Fig. 6. Responses of cyclic simple shear specimens subjected to variable amplitude harmonic loading.

Another variable amplitude harmonic test was performed by subjecting a torsional shear test specimen to 40 cycles of modulated harmonic loading of smoothly increasing and decreasing amplitude as shown in Figure 7. Examination of the figure shows that approximately 80% of the generated pore pressure developed in the first 20 cycles when the shear stress amplitude increased from one cycle to the next; the last 20 cycles, each of which had an amplitude that corresponded to a cycle in the first 20 cycles, produced much less pore pressure and the last 14 cycles, which had amplitudes less than 85% of the peak prior amplitude, produced essentially no additional pore pressure.

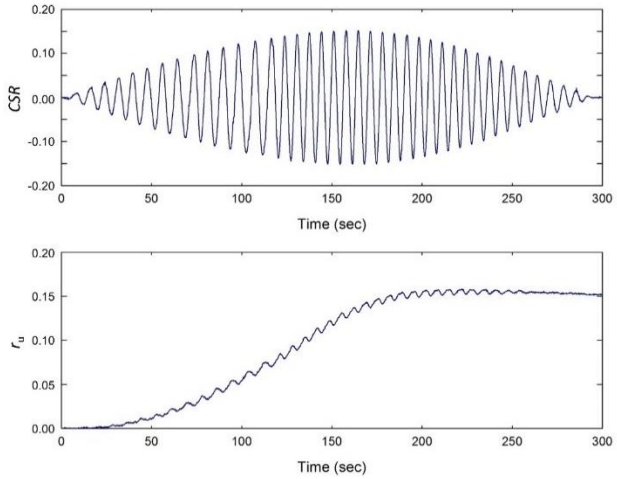

Fig. 7. Responses of cyclic simple shear specimens subjected to modulated harmonic loading (data courtesy of Fujen Ho, personal communication).

5.2 Transient Loading – Level-Ground Conditions

Actual earthquake ground motions are transient in nature and induce transient, highly irregular loading histories in potentially liquefiable soils. Transient ground motions are generally characterized by spectral content, either in terms of Fourier spectra or, more commonly, response spectra. Such characterizations typically do not capture ground motion duration well and do not capture the temporal variation of ground motion amplitude at all. For purposes of liquefaction hazard evaluation, peak acceleration and earthquake magnitude are also independent of temporal amplitude variation. Figure 8 shows the results of two cyclic torsional shear tests using the same loading history but reversed in time (i.e., run forward and backward). In both cases, pore pressures built up until the highest cyclic stress was reached and then remained essentially constant after that time. Cyclic shear strain amplitudes, however, were not noticeably influenced by peak past loading level. Peak and final pore pressures and cyclic strains were approximately 20% greater for the forward loading case.

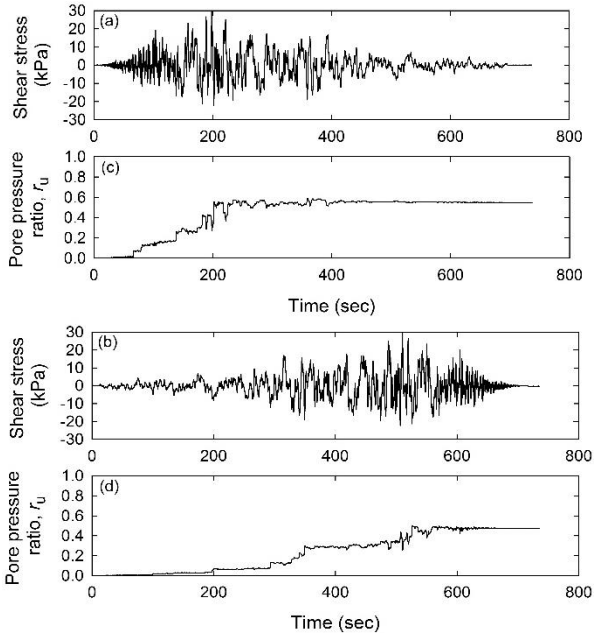

Fig. 8. Response of cyclic torsional shear specimens to the same loading history: (a) shear stress – forward loading, (b) pore pressure ratio – forward loading, (c) shear stress – reverse loading, (d) pore pressure ratio – reverse loading (data courtesy of Fujen Ho, personal communication).

To further investigate response to transient loading and to determine whether alternative intensity measures would be more suitable for liquefaction hazard evaluation, a cyclic simple shear testing program involving many transient loading histories was undertaken. The loading histories were obtained by a process intended to emphasize ground motion characteristics that would distinguish between the efficiencies of several evolutionary intensity measures. This involved identifying motions with combinations of amplitude, frequency content, duration, and phasing that differed significantly relative to each other. Figure 9(a) shows a scatter plot of two *IM*s computed from some 7000 recorded outcrop motions (V_{S30} > 360 m/sec) that span a wide range of magnitudes, distances, styles of faulting, basin depths, etc. [1]. There is a clear correlation between the two *IM*s but there are also motions that vary widely for one of the *IM*s with constant values of the other *IM*. Figure 9(b) shows examples of the four motions highlighted in Figure 9(a). Two of the motions have the same value of *PGA*/*MSF* but very different values of CAV_5 [19] and two have the same value of CAV_5 but very different values of *PGA*/*MSF*. Tests using shear stress histories based on motions with the same value of *PGA*/*MSF* but high and low values of CAV_5 that produced similar pore pressures would indicate that *PGA*/*MSF* was an efficient predictor of pore pressure generation (and hence liquefaction). An initial set of 15 motions developed to distinguish the relative efficiencies of *PGA*/*MSF*, Arias intensity, and

cumulative absolute velocity is shown in Figure 10. A supplemental set of six additional motions in which energy built up at different rates is shown in Figure 11.

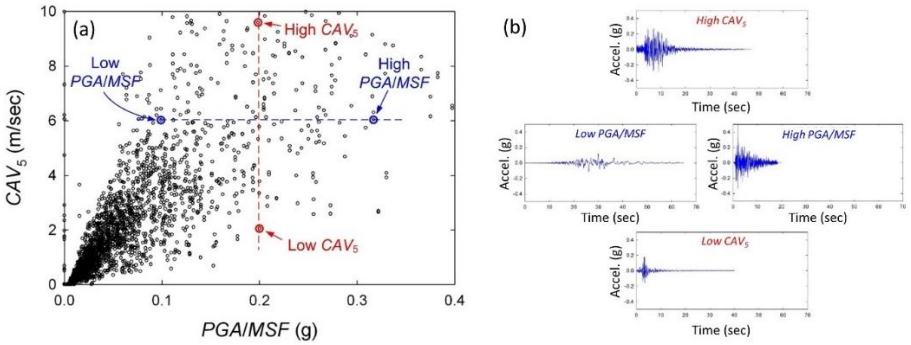

Fig. 9. Relationship between *PGA*/*MSF* and *CAV*5 for 7000 recorded outcrop motions highlighting motions with same *PGA*/*MSF* (red) and same *CAV*5 (blue) [1].

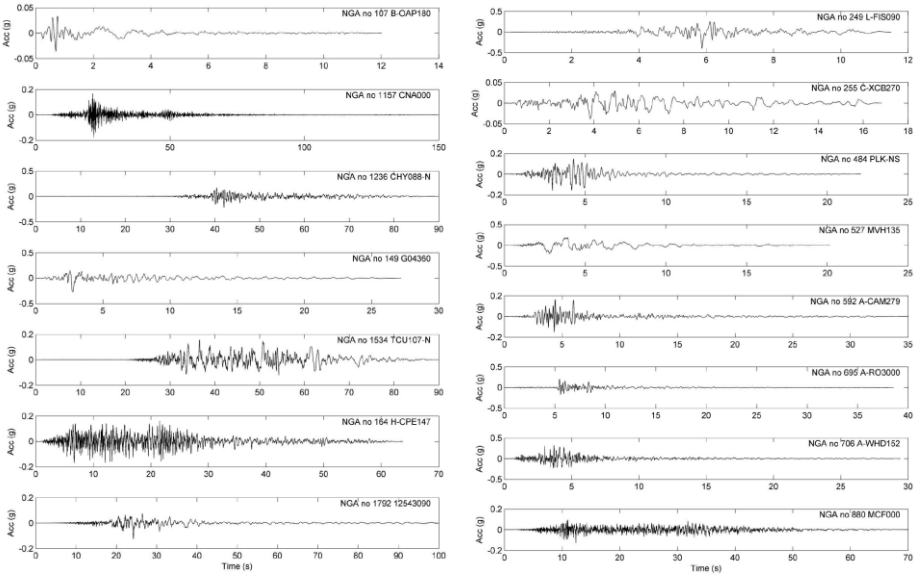

Fig. 10. Acceleration histories for 15 motions used to develop transient loading histories.

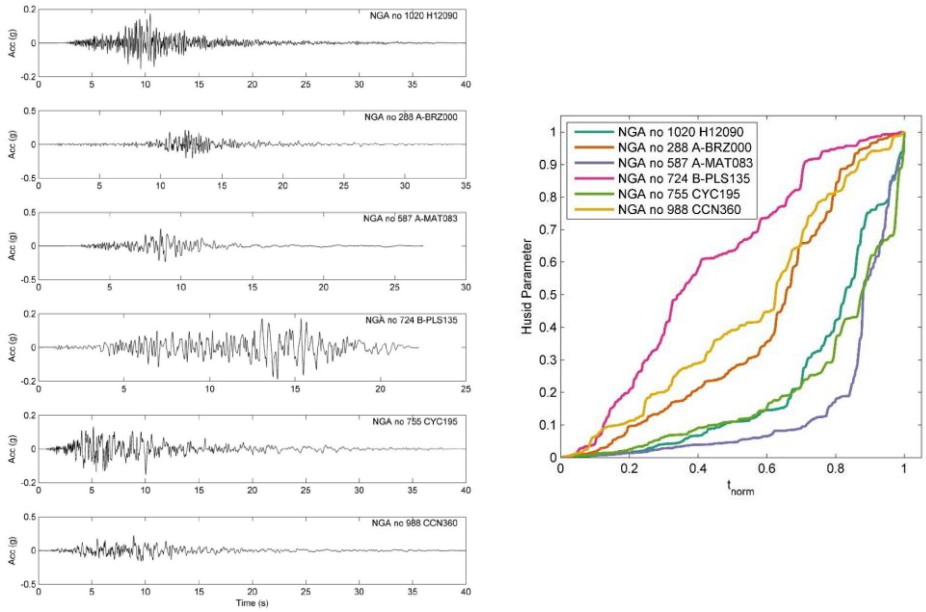

Fig. 11. (a) acceleration histories for six supplemental motions with different rates of energy buildup and (b) Husid plots illustrating rates of energy buildup.

The previously described motions were converted to shear stress histories by applying them at the base of an equivalent linear model of a 6-m-thick profile of medium dense (D_r = 55%) sand underlain by 1 m of cemented sand over a rigid base and extracting the shear stress history at a depth of 5 m; this profile corresponded to that of a prototype soil profile used in parallel centrifuge tests. The shear stress histories were applied to cyclic simple shear specimens prepared at relative densities ranging from 37-89% at 1/5 their actual rate to allow for accurate pore pressure measurement. Several of the tests were not used in subsequent analyses due to low (<0.90) *B*-values or apparent problems with the testing system. Because the loading system was not able to reproduce the input loading histories exactly, the measured shear stress histories were converted to input acceleration histories using a shear stress-based equivalent linear analysis program (Sideras, 2019) developed for the project.

An example of the measured response is shown in Figure 12. The measured pore pressure increases relatively quickly while the shear stress amplitude is increasing but stalls (e.g., from 138-142 sec) when cyclic stresses are lower than the peak past cyclic stress. Shear strains are small until the pore pressure ratio is nearly 1.0 and then become large; dilation-induced stiffening is clearly seen in the stress-strain and stress path curves.

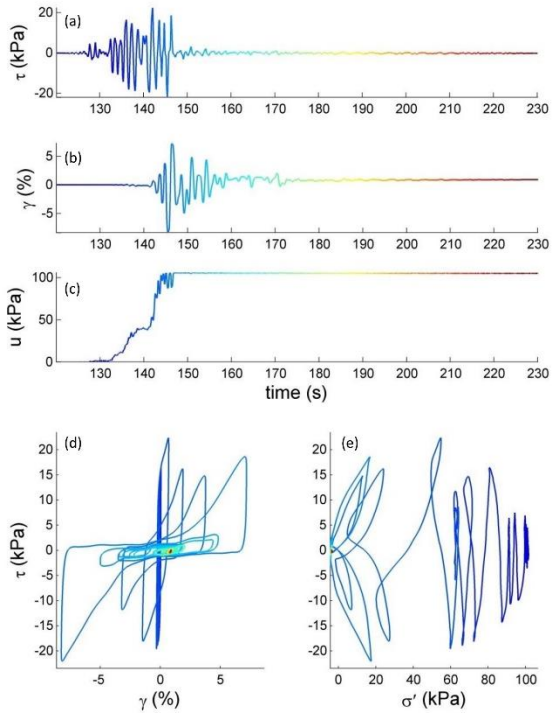

Fig. 12. Measured response of cyclic simple shear specimen subjected to transient loading history: (a) applied shear stress, (b) shear strain, (c) excess pore pressure, (d) stress-strain behavior, and (c) effective stress path.

The results of the transient loading tests were used to evaluate the relative efficiencies of four evolutionary liquefaction-related intensity measures. In order to do so, the measured pore pressure histories were modified by removing temporary reductions in pore pressure due to unloading and dilation; modified pore pressures were held constant during periods of measured pore pressure reduction. The evolutionary intensity measures examined were $PGA_M = PGA/MSF$, I_a, CAV, and CAV_5. Two versions of PGA/MSF were used – one in which MSF was obtained by correlation to number of loading cycles (Liu et al., 2001) and one in which MSF was also related to relative density through laboratory cyclic strength curves [5]. These IMs are referred to subsequently as $PGA_{M,L}$ and $PGA_{M,B}$, respectively. At a particular relative density, the modified pore pressure can be plotted as a function of the evolving intensity measure. The rate of pore pressure generation would increase with increasing intensity measure and decrease with increasing relative density. Because the pore pressure ratio is bounded by values of 0.0 and 1.0, the test data was interpreted in terms of the IM values from $r_u = 0.05$ up to the point of triggering (taken as $r_u = 0.99$). The relationship between the three variables (IM, D_r, and r_u) were found to be described well by the function

$$IM = \frac{1+\alpha_1}{1+\alpha_1 \cdot r_u^{\alpha_2}} \cdot \beta_1 \exp\left(\beta_2 D_r\right) \tag{11}$$

where α_1, α_2, β_1, and β_2 are coefficients obtained by regression for each evolutionary intensity measure. When the coefficients were determined based on the transient cyclic simple shear test results over the range of $0.05 < r_u < 0.99$, the standard deviations of the *IM* residuals were as indicated in Table 1. These values show considerable differences in the abilities of the different *IM*s to track pore pressure development up to and at the point of triggering.

Table 1. Coefficients and uncertainties for *IM* models.

IM	α_1	α_2	β_1	β_2	$\sigma_{\ln IM}$
$PGA_{M,L}$	0.2367	-1.228	0.07713	0.01441	0.31
$PGA_{M,B}$	0.3137	-1.082	0.1199	0.01404	0.24
I_a	0.0676	-2.658	0.06688	0.02624	0.82
CAV	0.372	-1.322	0.8443	0.01537	0.58
CAV_5	0.3167	-1.412	0.7972	0.01597	0.60

Discussion. The results of the transient loading tests indicate that PGA_M-based intensity measures are significantly more closely related to pore pressure generation during transient loading than the integral evolutionary intensity measures. Several factors appear to contribute to this finding:

1. The PGA_M-based intensity measures are based on the relative amplitudes of individual loading pulses without regard to the frequencies at which they occur.
2. Integral *IM*s are strongly influenced by frequencies and can increase significantly due to low frequency components of ground motions that would not produce significant shear strain (hence, pore pressure generation) in liquefiable soil layers.
3. The PGA_M-based intensity measures are nonlinearly related to the amplitudes of individual pulses in a way that emphasizes larger pulses and discounts (or ignores) the effects of small pulses that contribute little to pore pressure generation.
4. Integral *IM*s consider all pulses in proportion to their amplitudes and can have their values inflated by low-amplitude cycles that do not generate pore pressure.
5. PGA_M is more efficient at predicting the onset of phase transformation behavior after which pore pressures tend to increase more rapidly.

The relative manners in which PGA_M-based and integral evolutionary intensity measures account for irregular loading can be illustrated by considering the initial set of variable amplitude harmonic tests shown in Figure 13. Assuming the tests represent an element of soil at the same depth, shear stresses and *CSR* values would be proportional to accelerations in a simplified model analysis. Considering the tests with large pulses in the 4^{th}, 6^{th}, and 8^{th} cycles, which had similar relative densities, comparison of the shapes of the recorded pore

pressure responses (Figure 13b) and the $PGA_{M,B}$ (Figure 13f) and *CAV* (Figure 13g) show how much more closely $PGA_{M,B}$ correlates to pore pressure generation over the entire course of loading than *CAV*. As an integral parameter, *CAV* continues to increase from cycle to cycle with a relatively small jump during the large cycle. $PGA_{M,B}$, on the other hand, increases significantly during each large cycle and, as does the pore pressure, remains essentially constant thereafter.

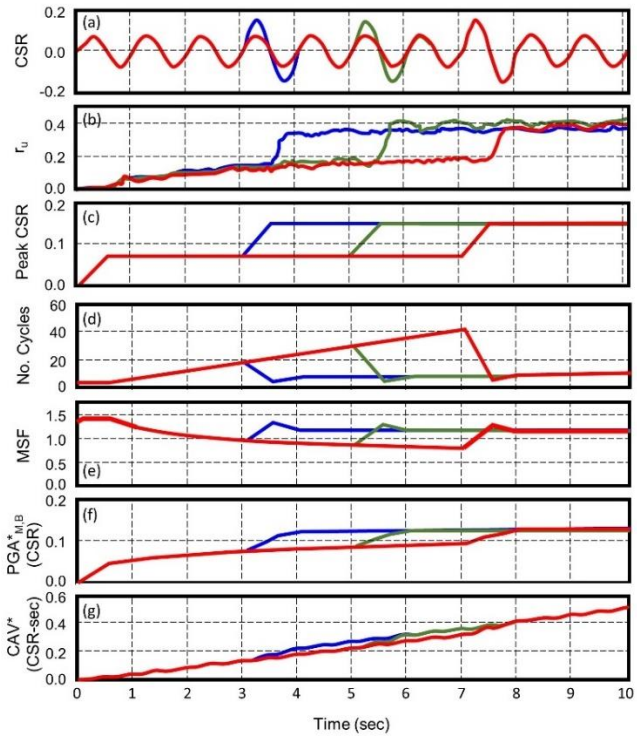

Fig. 13. Response histories of three cyclic simple shear specimens subjected to variable amplitude harmonic loading: (a) applied cyclic stress ratio, (b) generated pore pressure ratio, (c) peak cyclic stress ratio, (d) number of equivalent loading cycles, (e) magnitude scaling factor, (f) PGA^*_{MB} (computed as the quotient of (c) and (e)), and (g) CAV^* (computed using *CSR* rather than acceleration).

5.3 Transient Loading – Sloping Ground Conditions

In order to better understand the response of liquefiable soils to transient loading under conditions that commonly exist in the field, another series of cyclic simple shear tests were performed with transient loading superimposed on constant, static shear stresses (deLaveaga, 2016). The tests were performed at the Norwegian Geotechnical Institute

using two transient loading histories with very different temporal characteristics (Figure 14). The Palm Springs motion (MVH 135) was from the 1986 N. Palm Springs (**M**6.1) earthquake; this motion had a relatively short duration and was characterized by a few low-frequency pulses of acceleration that occurred early in the record. The Landers record (MCF 000) was from the 1992 Landers (**M**7.3) earthquake and had a long duration with many high-frequency pulses of similar amplitude.

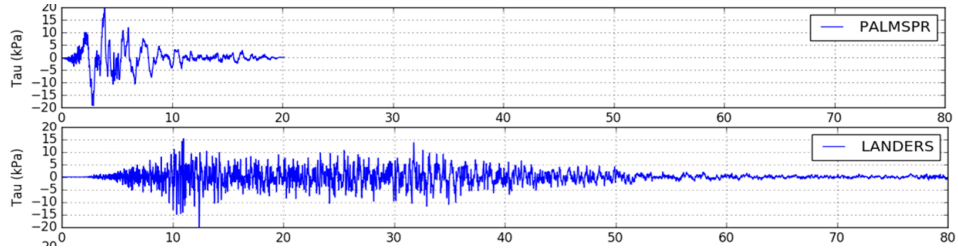

Fig. 14. Accelerograms for Palm Springs MVH 135 and Landers MCF 000 motions scaled to peak shear stresses of 20 kPa.

Tests with both uniform harmonic and transient loading were applied to the soil specimens and the transient loading tests were applied with nominal static stress ratios of 0.00, 0.05, 0.10, 0.15, and 0.20. Test specimens of Nevada sand were reconstituted by wet pluviation to relative densities ranging from approximately 35% to 70%. Tests were performed at 5% of the rate of the actual recorded earthquake motion. The responses of specimens subjected to the Palm Springs and Landers loading histories with different static shear stress levels are shown in Figures 15 and 16, respectively. Accounting for differences in relative densities, the specimens exhibited behavior generally consistent with that indicated in prior studies based on uniform harmonic loading (Figure 3). The specimens with relative densities in the range of 55-62% generated lower levels of excess pore pressure with increasing static shear stress levels, thus indicating K_α values greater than 1.0 and increasing with α.

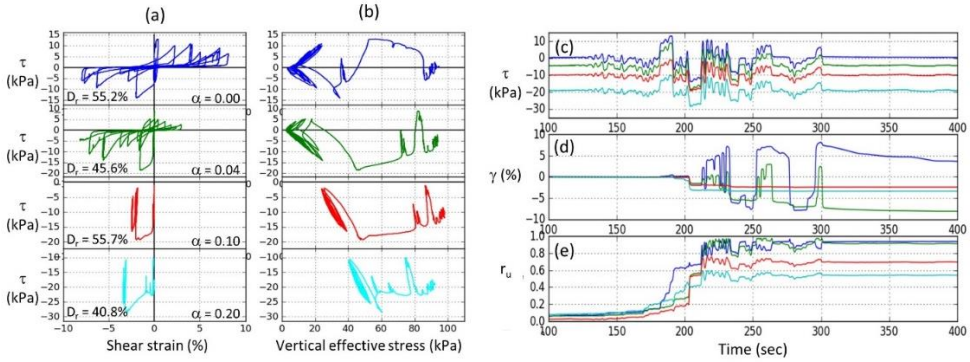

Fig. 15. Response of Nevada sand specimens to Palm Springs loading histories with constant *CSR* but different static shear stress levels: (a) stress-strain curves, (b) stress paths, (c) shear stress, (d) shear strain, and (e) pore pressure ratio.

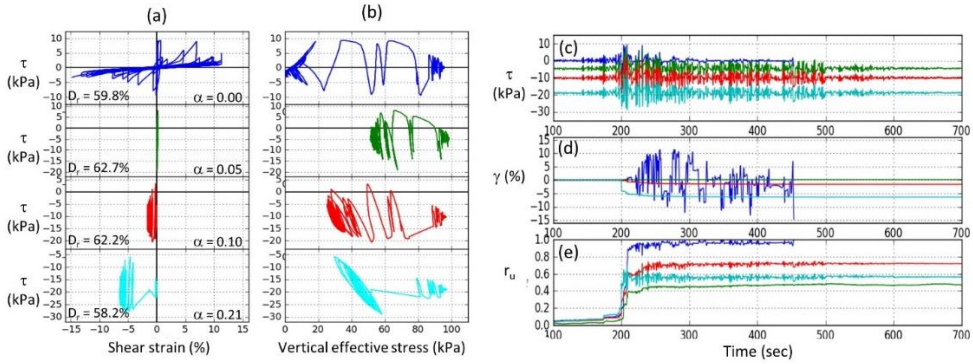

Fig. 16. Response of Nevada sand specimens to Landers loading histories with similar *CSR* but different static shear stress levels: (a) stress-strain curves, (b) stress paths, (c) shear stress, (d) shear strain, and (e) pore pressure ratio.

6 An Improved Intensity Measure for Triggering of Liquefaction

The variable amplitude and transient loading tests showed consistently that the generation of pore pressure was influenced by the temporal variation of ground motion amplitude, which is not accounted for in the intensity measures currently used in the evaluation of liquefaction potential. An intensity measure that does account for temporal variation as well as the amplitude and number of loading cycles would be beneficial in (a) the interpretation of liquefaction case histories in areas with nearby ground motion recordings, (b) the prediction of liquefaction for certain rupture scenarios in which repeatable temporal variations are expected (e.g., near-fault, forward and backward directivity cases), and (c) cases where ground motion hazards are defined in terms of ground motion histories (e.g., in the case of physics-based modeling).

Defining half-cycles as the periods between successive zero-crossings, the evolutionary form of $PGA_{M,B}$ at the j^{th} cycle of loading can be expressed as

$$PGA_{M,B,j} = \frac{PGA_j}{MSF_j} = PGA_j \left(\frac{N_j}{N_{ref}} \right)^b \tag{12}$$

where PGA_j is the peak absolute acceleration as of the j^{th} cycle, MSF_j is the magnitude scaling factor as of the j^{th} cycle, N_{ref} is the reference number of cycles (generally taken as

15), N_j is the number of equivalent cycles as of the j^{th} cycle, and b is an exponent that describes the slope of a cyclic strength curve. Assuming a linear relationship between damage and number of loading cycles,

$$N_j = \sum_{i=1}^{j} N_i = \sum_{i=1}^{j} \frac{1}{2}\left(\frac{pk_i}{0.65 PGA_j} \right)^{1/b} \tag{13}$$

where pk_i is the absolute value of the amplitude of the i^{th} local peak. This allows $PGA_{M,B}$ at the j^{th} cycle of loading to be written as

$$PGA_{M,B,j} = \frac{1}{0.65 N_{ref}^{b}} \left(\frac{1}{2} \sum_{i=1}^{j} pk_i^{1/b} \right)^{b} = C \left(\sum_{i=1}^{j} pk_i^{1/b} \right)^{b} \tag{14}$$

where C groups the constant terms for given values of N_{ref} and b. To allow more flexibility in modeling laboratory results, the two exponents on the right side of Equation (14) can be freed from their reciprocal relationship. To account for the observed order of cycles effect, in which cycles of increased amplitude produce relatively high increments of pore pressure and cycles of amplitude lower than the prior peak (absolute) amplitude between zero crossings (i.e, the *PPA*) produce small increments of pore pressure, a peak ratio factor, r, that amplifies the effects of peaks that define new *PGA* values and reduces the effects of peaks that are preceded by a higher peak. This allowed a liquefaction triggering intensity measure to be defined as

$$IM_L = \left[\sum_{i=1}^{j} \left(pk_i \cdot \frac{2}{1 + \left(\frac{pk_i}{PPA} \right)^{\theta_3}} \right)^{\theta_2} \right]^{\theta_1} \tag{15}$$

The peak ratio factor ranges from zero to 2 and takes on values less than 1.0 for peaks preceded by a higher peak (i.e., $pk_i < PPA$), greater than 1.0 for peaks that exceed all prior peaks ($pk_i > PPA$), and equal to 1.0 for peaks equal to the prior peak ($pk_i = PPA$). The coefficient, θ_3, controls the rate at which r changes with pk_i / PPA. Examination of Equation (c) shows that $\theta_1 = b$ and $\theta_2 = 1/b$ in the Boulanger and Idriss formulation; that formulation would produce $b = 0.236$ for $(N_1)_{60,cs} = 15$ blows/ft. The values of the coefficients, θ_1-θ_3, were determined through a process of constrained optimization with the constraints set to avoid convergence to coefficient values that differed greatly from those

based on laboratory data (Boulanger and Idriss, 2014). The coefficients θ_1 and θ_2 were constrained to lie within ranges of 0.15 to 0.55 and 0.7/ θ_1 to 1.4/ θ_1, respectively; θ_3 was constrained to being between -5.0 and zero. Using an objective function defined as the sum-of-squared-errors in $\ln IM_L$, values of $\theta_1 = 0.298$, $\theta_2 = 2.53$, and $\theta_3 = -2.91$ were obtained. The uncertainty in IM_L was characterized by $\sigma_{\ln IM_L} = 0.16$, which is significantly lower than the corresponding values for the other evolutionary *IM*s listed in Table 1.

Figure 17 shows how the peak ratio factor discounts the contributions of pulses preceded by larger pulses and amplifies the contributions of those that represent new peak loadings. Note that Seed et al. (1975) assumed that accelerations less than 30% of the *PGA* do not contribute to N_{eq}; Sassa and Yamazaki (2017) did not count shear stresses less than 60% of the peak shear stress toward their effective number of stress cycles. Examination of transient test data showed that pore pressure ratios at the first exceedance of 30% of the peak shear stress were generally less than 0.1 but could be as high as 0.3 in some tests. The peak ratio factor shown in Figure 17 provides a smooth and continuous variation with the evolving *PPA* as opposed to peak values for the entire motion.

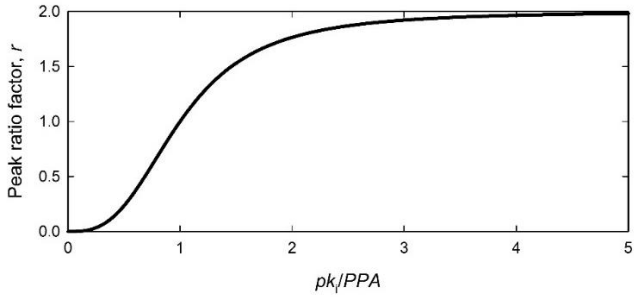

Fig. 17. Variation of peak cycle weighting factor applied to individual cycles in proposed intensity measure.

7 Toward an Improved K_α Adjustment Factor

The effect of static shear stress on the triggering of liquefaction under transient loading can be quantified by a K_α term (Equation 1) but care must be taken in the definition of that term due to the transient nature of actual earthquake motions. For uniform harmonic loading, the *CRR* terms can be defined using the peak shear stress, which is the same for all loading cycles. For transient loading, however, the amplitudes of individual loading pulses vary over the duration of the loading, which complicates definition of K_α. In this study, the evolving magnitude-corrected cyclic stress ratio could be computed at the point at which liquefaction was observed to have been triggered, i.e., as

$$CRR_{\alpha,state} = CSR_M(t_{state}) = \frac{CSR(t_{state})}{MSF(t_{state})} = \frac{[\tau_{\max}(t_{state}) - \tau_{static}]/\sigma'_{vo}}{f[N_{eq}(t_{state})]} \quad (16)$$

where t_{state} is the time of at which some state of interest (typically the triggering of liquefaction) is reached and $f[N_{eq}(t_{state})]$ is the *CRR* scaling factor (analogous to *MSF*) at time, t_{state}, obtained using a cycle counting-based procedure applied to the cyclic portion of the loading history (i.e., to $\tau_{\max}(t) - \tau_{static}$). The transient load testing program for sloping ground conditions had a relatively small number of tests in which initial liquefaction was actually reached and those tests were all conducted at α-values less than about 0.05. In order to gain insight into the effects of static shear stress over a broader range of conditions relevant to practice, the finding of close correlation between intensity measures at the point of phase transformation $(r_u \approx 0.6)$ and $r_u \approx 1.0$ for level-ground transient loading [32] was used to define $CRR_{\alpha,0.6}$ (i.e., CRR_α for the state of $r_u = 0.6$). This roughly doubled the number of data points and extended the range of α out to 0.21. A smooth function quadratic in both α and D_r was then fit to the data as illustrated in Figure 18. This function can then be used to define K_α for the state of interest, i.e.,

$$K_{\alpha,0.6} = \frac{CSR_{\alpha,0.6}}{CSR_{\alpha=0,0.6}} \quad (17)$$

for which curves at different relative densities are shown in Figure 19.

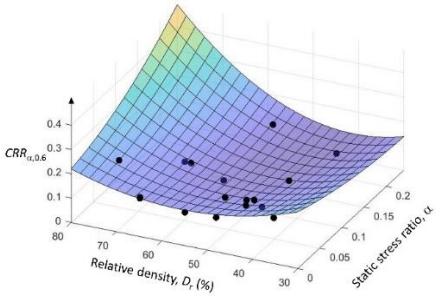

Fig. 18. Smooth function fit to cyclic resistance ratios corresponding to the state of $r_u = 0.60$.

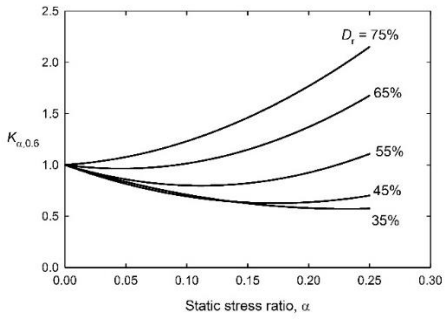

Fig. 19. Curves of $K_{\alpha,0.6}$ from transient loading tests with Palm Springs motion for different soil densities.

The $K_{\alpha,0.6}$ curves of Figure 19, while not a substitute for K_α, provide insight into how improved models might be developed. The curves can be seen to be generally consistent with those in Figure 3. They show $K_\alpha < 1.0$ for loose sands and $K_\alpha > 1.0$ for medium dense to dense sands. The shapes of the curves, however, differ from those shown in Figure 3 in that they are all concave upward, i.e., all show increasing K_α at large values of α for all densities. This behavior appears to be reasonable given the differences in loading between the uniform loading histories used to develop the relationships shown in Figure 3 and the transient loading upon which the curves shown in Figure 19 are based. As the static shear stress is increased in a series of uniform harmonic loading cycles, the amplitudes of the stress reversals decreases but the number of stress reversals remains unchanged until dropping to zero instantaneously when α exceeds *CSR*. Under transient loading, however, both the amplitude and the number of stress reversals decrease with increasing static shear stress. As a result, the effects of static shear stress should appear earlier and more intensely for transient loading than for uniform loading.

8 Summary and Conclusions

Improved understanding of the mechanics of liquefiable soil behavior has led to the development of improved tools for analyzing the response of liquefiable soil profiles in recent years. Advanced numerical models employing well-documented, validated constitutive models are capable of representing important behaviors of liquefiable soils up to and, increasingly, after the triggering of liquefaction. These tools allow engineers to visualize the mechanisms by which pore pressures generate, redistribute, and dissipate, and by which resulting deformations develop. The insight and understanding gained from these analyses can be invaluable and their use in practice will continue to increase.

At the same time, the depositional complexities of many soil profiles prevent subsurface characterization so complete that all behaviors can be anticipated or quantified even in the most capable of numerical models. Both the mechanical and hydraulic response of a liquefiable soil profile can be sensitive to the presence of thin layers or lateral inhomogeneities that are not captured by typical subsurface investigations. As a result, the use of empirical procedures for evaluating liquefaction potential and its consequences will remain an important part of geotechnical earthquake engineering practice. Empirical procedures have evolved and improved as understanding of liquefiable soil behavior has developed and as more case histories have been documented in large and small earthquakes around the world.

Empirical models for the triggering of liquefaction require characterization of demand and capacity, i.e., of the loading imposed on liquefiable soils and the resistance of those soils to the generation of high pore pressures. The great majority of liquefaction research to date has focused on liquefaction resistance with less attention being paid to loading. The laboratory tests that have elucidated important behaviors that cannot be obtained from available case histories have represented earthquake loading by harmonic shear stresses of

constant amplitude, and empirical models are based on the concept of representing the transient, irregular nature of actual earthquake loading by a number of equivalent uniform harmonic stress cycles. This was due, in large part to the common use of pneumatic loading systems driven by function generators available at the time. With the advanced control systems of modern laboratory testing equipment now available, however, that restriction has been overcome and it is possible to apply loading more representative of actual earthquake loading and to understand how liquefiable soils respond differently to such loading.

This paper presents some of the results of cyclic simple shear tests in which loading histories representative of actual earthquake loading are applied. The intent of the tests was to help identify optimal intensity measures for evaluation of liquefaction hazards, and to develop data that could be used by constitutive modelers to validate or improve their models. Tests were performed to simulate level-ground conditions with a large number of loading histories based on different recorded ground motions, and to simulate sloping ground conditions with two motions. The results of the tests have led to several significant conclusions.

1. The generation of excess pore pressure in liquefiable soils is more closely related to the number and amplitude of the individual stress pulses that make up a loading history than to the duration of that history. Thus, the potential for time-integrated intensity measures such as Arias intensity or cumulative absolute velocity to be efficient predictors of liquefaction triggering appears to be limited.
2. The manner in which pore pressures develop under transient loading is influenced by the order of the stress pulses imposed on the soil. Thus, commonly used intensity measures and cycle-counting procedures, which treat all pulses equally based solely on their amplitudes, are limited in their ability to represent pore pressure generation.
3. The incremental pore pressure generated by an individual stress pulse is strongly influenced by the amplitude of that pulse relative to the past peak amplitude. If the pulse is preceded by a larger pulse, it will generate a significantly smaller increment of pore pressure than if it had not. This leads to the irregular generation of pore pressures under earthquake loading in which large increments of pore pressure are associated with stress pulses that exceed all preceding pulses followed by nearly constant pore pressures between those pulses.
4. The transient testing performed in this investigation supports the concept of a new intensity measure, IM_L, that explicitly considers the order of cycles in a ground motion. It therefore offers the potential to better distinguish between motions of short and long duration, motions of forward and backward directivity, and motions with different source rupture characteristics. In the context of empirical procedures, such an intensity measure can be used with recorded ground motions in the vicinity of liquefaction case histories to better characterize the loading imposed on the soil in those case histories.
5. The presence of static shear stresses, as occur under sloping ground conditions or in the vicinity of structures, appears to influence pore pressure generation and

liquefaction triggering in a manner generally consistent with that exhibited in tests involving uniform harmonic loading. However, the relationship and interaction between transient shear stress histories and static shear stresses is significantly different than for uniform harmonic loading, particularly when static stresses are high relative to cyclic stresses, a condition for which little test data is currently available.

6. Additional testing with transient loading is needed. The investigations described in this paper were limited and exploratory and used only uniformly-graded clean sand. Additional testing is needed with a broader range of soils (different grain size distributions, fines contents, fines plasticities) and broader ranges of relative densities and loading amplitudes. Tests that extend beyond the point of triggering, particularly tests with static shear stresses, will also be useful to better understand the development of large strains and to identify intensity measures that predict those strains efficiently and sufficiently. Such intensity measures can be expected to improve empirical models for prediction of the consequences of liquefaction.

Acknowledgments

The research described in this paper was supported by the National Science Foundation (Award 0936408). The efforts of Masters students Stephanie Abegg and Katie deLaveaga with analytical and experimental work is greatly appreciated; Ms. deLaveaga's work at NGI was supported by a Valle Foundation fellowship from the University of Washington. The use of NGI testing equipment and the assistance of NGI personnel, particularly Dr. Brian Carlton and Dr. Amir Kaynia, is also greatly appreciated.

References

1. Abegg, S. (2010). "Identification of optimal evolutionary intensity measures for evaluation of liquefaction hazards," Masters thesis, University of Washington, 185 pp.
2. Azeiteiro, R.N., Coelho, P.A.L.F., Taborda, D.M.G., and Grazina J.C. (2015). "Dissipated energy in undrained cyclic triaxial tests," Proceedings of the 6th International Conference on Earthquake Geotechnical Engineering, Christchurch, New Zealand, 1–4, paper no. 220.
3. Azeiteiro, R.N., Coelho, P.A.L.F., Taborda, D.M.G., and Grazina J.C. (2017). "Energy-based evaluation of liquefaction potential under-non-uniform cyclic loading," Soil Dyn. Eq. Eng., 92, 650-665.
4. Boulanger, R.W. (2003) "Relating Kα to relative state parameter index". J Geotech Geoenv. Eng., ASCE 129(8) 770–773.
5. Boulanger, R.W., and Idriss, I.M. (2014). "CPT and SPT based liquefaction triggering procedures," Rep. No. UCD/CGM-14/01, Center for Geotech. Modeling, U.C. Davis, Davis, Calif., 138 pp.
6. Cetin, K.O. and Bilge, H.T. (2015). "Stress scaling factors for seismic soil liquefaction engineering problems: A performance-based approach," Perspectives on Earthquake Geotechnical Engineering, A. Ansal and M. Sakr, eds., Springer Int. Pub., 113-139.
7. deLaveaga, K.M. (2016). "Slope effects on liquefaction potential and pore pressure generation in earthquake loading," Masters thesis, University of Washington, 113 pp.

8. De Alba, P., Seed, H.B., and Chan, C.K. (1976). “Sand liquefaction in large-scale simple shear tests,” J. Geotech. Eng. Div., ASCE, 102(GT9), 909-927.
9. Dobry, R., Ladd, R., Yokel, F., Chung, R., and Powell, D. (1982). “Prediction of pore water pressure buildup and liquefaction of sands during earthquakes by the cyclic strain method.” NBS Building Science Series 138, Nat. Bur. Stand., U.S. Dept. of Commerce.
10. Green, R. A., Mitchell, J. K., and Polito, C. P. (2000). “An Energy-Based Excess Pore Pressure Generation Model for Cohesionless Soils.” Proc. The John Booker Memorial Symposium – Developments in Theoretical Geomechanics (D.W. Smith and J.P. Carter, eds.), A.A. Balkema, Rotterdam, the Netherlands, 383–390.
11. Green, R.A. and Terri, G.A. (2005). “Number of equivalent cycles concept for liquefaction evaluations – revisited,” J. Geotech. Geoenv. Eng., 131(4) 477-488.
12. Hancock, J. and Bommer, J.J. (2005). “The effective number of cycles of earthquake ground motion,” Earthquake Eng. Struct. Dyn., 34, 637–664.
13. Idriss, I. M. (1999). An update to the Seed-Idriss simplified procedure for evaluating liquefaction potential, in Proceedings, TRB Workshop on New Approaches to Liquefaction, Pub. No. FHWARD-99-165, Fed. Hwy. Admin.
14. Ishihara, K. and Yasuda, S. (1973). “Sand liquefaction under random earthquake loading conditions,” Proc., 5th World Conf. Eq. Eng., Rome.
15. Ishihara, K. and Yasuda, S. (1975). “Sand liquefaction in hollow cylinder torsional under irregular excitation,” Soils Found. 15(1) 45-59.
16. Kayen, R.E. and Mitchell, J.K. (1997). “Assessment of liquefaction potential during earthquakes by Arias intensity,” J. Geotech. Geoenv. Eng., ASCE 123(12) 1162-1174.
17. Kishida, T. and Tsai, C.-C. (2014). “Seismic demand of the liquefaction potential with equivalent number of cycles for probabilistic seismic hazard analysis,” J. Geotech. Geoenv. Eng., ASCE,140(3) 1-14.
18. Kokusho, T. (2013). “Liquefaction potential evaluations: energy-based method versus stress-based method,” Can. Geotech. J., 50, 1088-1089.
19. Kramer, S.L. and Mitchell, R.A. (2006). “Ground motion intensity measures for liquefaction hazard evaluation,” Earthquake Spectra, 22(2) 413-438. doi.org/10.1193/1.2194970
20. Kwan, W.S. (2015). Laboratory investigation into evaluation of sand liquefaction under transient loadings. PhD dissertation, University of Texas, Austin, TX.
21. Kwan, W.S., Sideras, S.S., Kramer, S.L. and El Mohtar, C. (2017). “Experimental database of cyclic simple shear tests under transient loadings,” Earthquake Spectra, 33(3), 1219-1239. doi.org/10.1193/093016eqs167dp
22. Liang, B.L., Figueroa, J.L., and Saada A.S. (1995). “Liquefaction under random loading: unit energy Approach,”. J. Geotech. Eng.,121(11) 776–81.
23. Liu, A.H., Stewart, J.P., Abrahamson, N.A. and Moriwaki, Y. (2001). “Equivalent number of uniform stress cycles for soil liquefaction analysis,. J. Geotech. Geoenv. Eng., ASCE, 127(12) 1017-1026.
24. Miner, M. A. (1945).“Cumulative damage in fatigue.” Trans. ASME 67, A159–A164.
25. Palmgren, A. (1924). “Die lebensdauer von kugella geru.” ZVDI, 68(14) 339–341.
26. Pan, K., and Yang, Z.X. (2018). “Effects of initial static shear on cyclic resistance and pore pressure generation of saturated sand,” Acta Geotechnica, 13(2) 473–487.
27. Polito, C., Green, R.A., Dillon, E., and Sohn, C. (2013). “Effect of load shape on relationship between dissipated energy and residual excess pore pressure generation in cyclic triaxial tests,” Can. Geotech. J., 50(11) 18–28.

28. Sassa, S. and Yamazaki, J. (2017). “Simplified liquefaction predictions and assessment method considering waveforms and durations of earthquakes, J. Geotech. Geoenv. Eng., 143(2):04016091.
29. Seed, H.B., Idriss, I.M., Makdisi, F., Banerjee, N. (1975). “Representation of irregular stress time histories by equivalent uniform stress series in liquefaction analysis,” Earthquake Eng. Res. Cen. Rep. EERC 75-29, University of California, Berkeley.
30. Seed, R.B. and Harder, L.F., Jr (1990). “SPT-based analysis of cyclic pore pressure generation and undrained residual shear strength” Proc. H. Bolton Seed Mem. Symp..
31. Shome, N. and Cornell, C.A. (1999). “Probabilistic seismic demand analysis of nonlinear structures,” Report RMS-35, Dept. Civil Eng., Stanford Univ., 320 pp.
32. Sideras, S.S. (2019). “Evolutionary intensity measures for more accurate and informative evaluation of liquefaction triggering,” Ph.D. Dissertation, University of Washington, 717 pp.
33. Tatsuoka, F. and Silver, M.L. (1981). “Undrained stress-strain behavior of sand under irregular loading,” Soils Found., 21(1) 51-66.
34. Vaid, Y.P., Stedman, J.D., and Sivathayalan, S. (2001). “Confining stress and static shear effects in cyclic liquefaction,” Can. Geotech. J., 38(3) 580–591. doi:10.1139/t00-120.
35. Wang, J.N. and Kavazanjian, E. (1989). “Pore pressure development during non-uniform cyclic loading,” Soils Found., 29(2) 1-14.